npj | biofilms and microbiomes

Article

Published in partnership with Nanyang Technological University

https://doi.org/10.1038/s41522-025-00742-6

Di (2-ethylhexyl) Phthalate decrease pregnancy rate via disrupting the microbe-gut-hypothalamic-pituitary-ovarian axis in mice

Linjie Xu[1,2] ✉, Jun Yan[1,2], Tingting Yin[1,2], Yingzi Pan[1], Min Chen[1], Xinyan Wang[1], Lan Wu[1] & Hongjuan Ding[1] ✉

Di (2-ethylhexyl) Phthalate (DEHP), a widely used plasticizer and endocrine disruptor, poses risks to human health, particularly reproductive function. Using a mouse model, we investigated how DEHP exposure impacts the hypothalamic-pituitary-ovarian (HPO) axis through gut microbiome disruption. DEHP decreased pregnancy rates by impairing ovarian function, activating hypothalamic astrocytes, and increasing neuregulin 1 (NRG1) expression. NRG1 binding to astrocyte ErbB2 receptors elevated prostaglandin E2 (PGE2) and gonadotropin-releasing hormone (GnRH), disrupting HPO axis homeostasis. Additionally, DEHP altered gut microbiota, destabilized microbial networks, and impacted β-glucuronidase-related taxa, leading to hormone fluctuations and reduced fertility. This study highlights gut microbiome perturbations as a novel mechanism linking DEHP exposure to reproductive dysfunction. Our study provides novel insights concerning perturbations of the gut microbiome and HPO axis and their functions as a potential new mechanism by which DEHP exposes interferes with the reproductive function-related human health.

Di (2-ethylhexyl) Phthalate (DEHP) is a widely utilized organic compound within the plastics industry and most commonly serving as a plasticizer for polyvinyl chloride (PVC) products[1]. Researches have demonstrated that DEHP can leach out from PVC materials that resulting in significant acute exposure levels in greenhouse vegetables, airborne dust, and even medical blood transfusion tubes[2–4]. Due to the extensive use of phthalates in food processing and packaging, dietary intake of processed foods may be a major source of human exposure to phthalates[5]. DEHP has been classified as a Group 2B carcinogen by the International Agency for Research on Cancer (IARC), an entity affiliated with the World Health Organization in 2017. Considering that DEHP has a wide range of uses and is frequently found in soil, rivers and agricultural products, its health effects are of concern[6]. Epidemiological investigations have revealed a robust association between occupational DEHP exposure and diminished fecundity, heightened rates of pregnancy loss, diminished estrogen concentrations, and disrupted ovulatory patterns, among various adverse outcomes related to reproductive health[7]. Despite it has been reported that DEHP can disrupt the reproductive functions in both women and men previously[8,9], the precise mechanisms are still relatively poorly understood.

Gut microbiome, functioning as the human acquired second genome, can transform environmental, dietary and endogenous molecules into microbial-derived functioning metabolites, which allow their communication with various organs, a phenomenon referred to as the gut-organ axis[10,11]. The communications between the gut-associated microbiota and host assumes a pivotal function in upholding host well-being, but these interactions are extremely easy to be disturbed by environmental factors, which are drivers in many diseases[12]. The gut microbiota exhibits heightened vulnerability to exogenous stressors, in particular the environmental pollutants serving as potent disruptors of the balance within the intestinal microbial community[13]. Altered microbiota structures were recently reported in most of the diseases caused by environmental toxicological factors, which always provoke pathophysiologies in vital human organs[14]. The primary route of human exposure to environmental pollutants is through food intake, which establishes a direct pathway for environmental pollutants to interact with gut microbes[15]. It has been reported that dietary exposure to environmental pollutants such as DEHP could significantly shift the diversity and composition in the gut microbiota, driving metabolic or physiological abnormalities in host[16–18]. However, reveal mechanisms in

[1]Department of Obstetrics, Women's Hospital of Nanjing Medical University, Nanjing Women and Children's Healthcare Hospital, Nanjing, Jiangsu, PR China. [2]These authors contributed equally: Linjie Xu, Jun Yan, Tingting Yin. ✉e-mail: linjiexu@njmu.edu.cn; njdinghj@163.com

which how environmental pollutants-induced gut microbiota contributes to host lesion is still a daunting task given the complexity of microbiota-gut-organ interactions, and the dependence of those interactions on environmental conditions.

Hypothalamic-pituitary-ovarian (HPO) axis represents the predominant and fundamental axis governing female neuroendocrinology and reproductive processes[19], which controls secretion levels of key regulators of reproductive function such as gonadotropins, gonadotropin-releasing hormone (GnRH) and estrogen. Any disruptions in HPO axis can lead to aberrant physiological conditions, encompassing endocrine disturbances and reproductive disorders. GnRH neurons and astrocytes in the hypothalamus play a crucial role in regulating GnRH secretion[20,21]. Neuregulin 1 (NRG1) can activate a network of ligand-receptor interactions by binding to the human epidermal growth factor receptor 2 (ErbB2), which subsequently triggers the release of prostaglandin E2 (PGE2) from hypothalamic astrocytes[22]. PGE2 can be further involved in neuromodulation within the reproductive system, particularly affecting the neuroendocrine regulation of GnRH release[23]. This intricate process serves a crucial regulatory role in the reproductive system and is able to maintain the normal reproductive function. Despite it has been reported that exposure to DEHP induces disturbances in the HPO axis in rats, thereby exerting a detrimental impact on the reproductive system[24,25], the extent and precise molecular mechanisms to which DEHP is involved in regulating GnRH release through the activation of astrocytes remain incompletely understood.

Notably, imbalances in gut microbiome equilibrium have the potential to trigger reproductive dysfunction via reciprocal gut–hypothalamus signaling pathways, predominantly facilitated by metabolites or neuroregulatory agents synthesized by gastrointestinal microorganisms[26,27]. Such as probiotics colonize the gut plays a beneficial role in alleviating HPO axis functioning disorders in polycystic ovary syndrome (PCOS) patients[28], suggesting that the beneficial gut microbiota can contribute to the maintenance of HPO axis homeostasis. However, there exists limited insight regarding whether and in what manner DEHP exposure elicits alterations to the gut microbiota's community structure, as well as the mechanisms through which perturbations in gut microbial composition mediate the disruptions to the HPO axis brought about by DEHP exposure.

In the current study, a sequence of experimental procedures was conducted to assess the effects of DEHP on reproductive function, in which the mice were orally exposed to DEHP over a short-term period of 16 days or a long-term duration of 32 days. The effects of DEHP on hypothalamus astrocytes secreted neuregulin, pituitary-related hormone, ovarian pathology, the composition and function of the intestinal microbiome, and the reproductive ability of mice were evaluated. This design allowed us to disentangle the role of the microbe-gut-HPO axis in DEHP-mediated reproductive toxicity. We hypothesized that the impaired reproductive function induced by DEHP exposure was caused by disruption of microbe-gut-hypothalamic-pituitary-ovarian (microbe-gut-HPO) axis homeostasis. Mechanistically, such effects could be driven by introduce DEHP enters the blood as an endocrine disruptor to directly impair the functions of hypothalamus and ovary, leading to the disordered secretion of HPO axis-related hormones, and further enforced by shifting the composition and functioning of the existing resident gut-related microbiome to indirectly enhance the damage for the HPO axis homeostasis, which can result the decrease of pregnancy rate. These findings will provide reliable evidence and novel insight of the potential detrimental risks of DEHP to female reproductive health, as well as potential therapeutic avenues.

Results

Residual effects of Di (2-ethylhexyl) Phthalate in different tissues of mice

To estimate possible disruption effects of DEHP on ovarian function and fertility of mice, we first used LC-MS to determine the contents of DEHP in different tissues of mice. We found that DEHP residues could be detected in the tissues of intestine, blood, and hypothalamus of mice both after short- and long-term exposure to DEHP, suggesting systemic exposure and potential bioaccumulation in these tissues (Fig. 1A). Although no

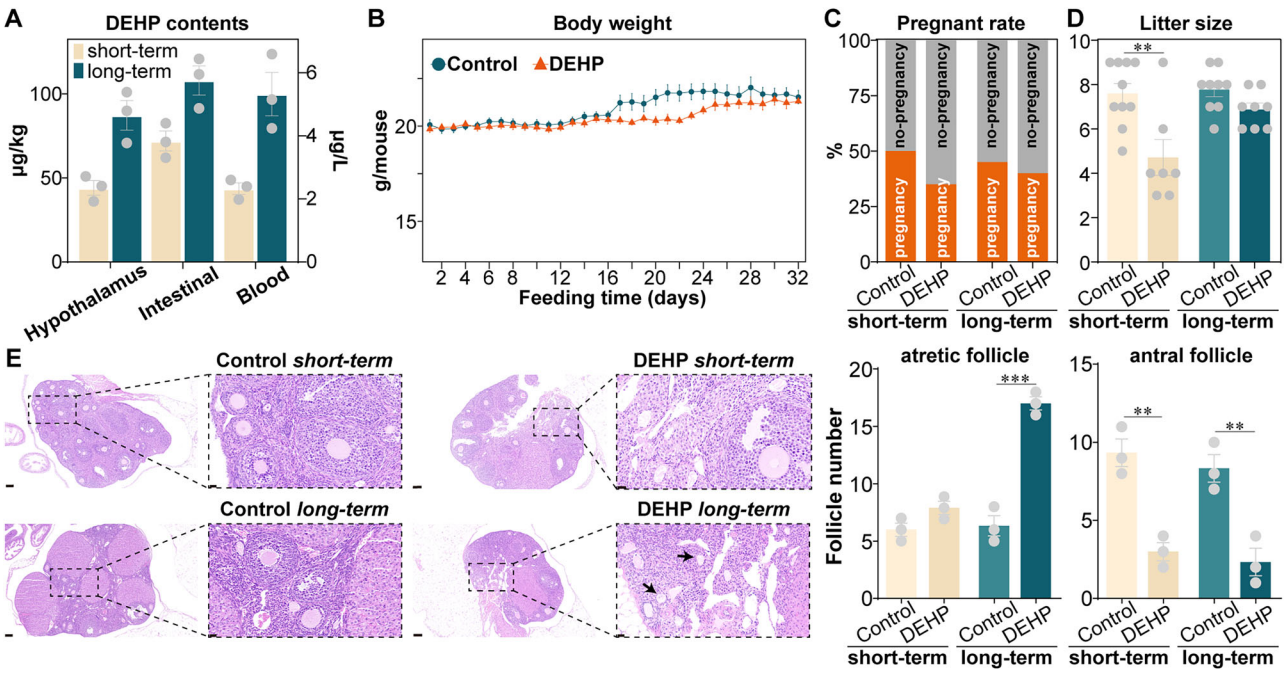

Fig. 1 | Residues of DEHP and its effects on fertility and ovarian function in mice. **A** The DEHP residues in the blood (μg/L), hypothalamus and intestine (μg/kg) of mice. **B** Alterations in body weight observed in mice exposed to DEHP. **C** Pregnancy rate in mice subjected to short-term and long-term DEHP treatments. **D** Litter size in mice subjected to short-term and long-term DEHP treatments. For the short-term DEHP treatment group, the Mann–Whitney *U* test was used, while for the long-term DEHP treatment group, the Student's *t* test was applied (**$p < 0.01$). **E** Histological examination (H.E. staining) of ovarian tissue and a chart of the follicle count ($n = 3$, Student's *t* test, **$p < 0.01$; ***$p < 0.001$). The image on the right represents a magnified view of the region enclosed by the black box in the image on the left. The black arrows indicate the location of atretic follicles. Scale bar for the left image: 100 μm. Scale bar for the right image: 20 μm.

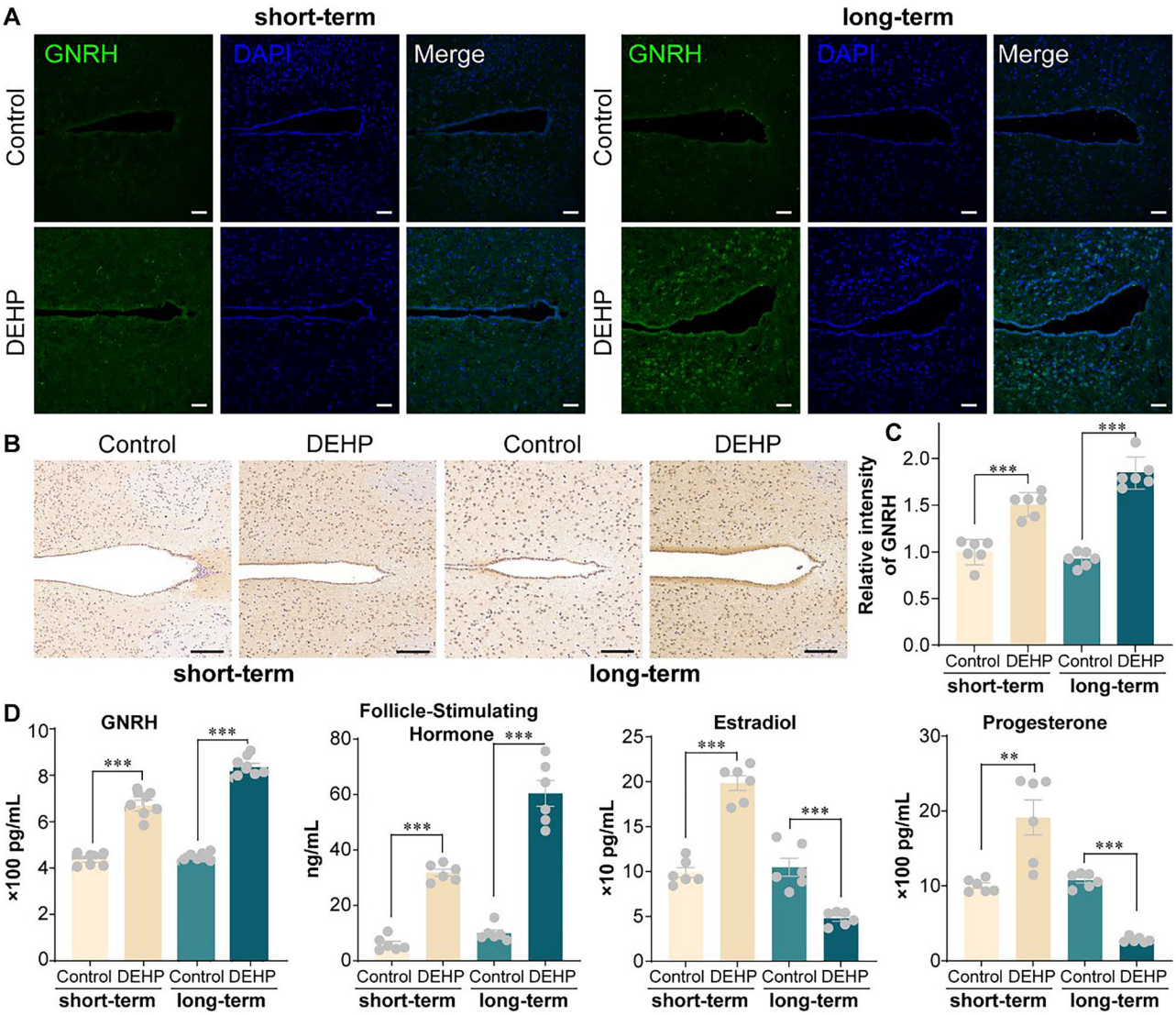

Fig. 2 | DEHP disrupted the HPO axis regulatory homeostasis. A Representative graphs illustrating the immunofluorescence of GnRH in various DEHP treatment groups and control groups. Scale bars: 50 μm. **B** Representative graphs demonstrating immunohistochemical analysis. Scale bars: 100 μm. **C** Statistical plots illustrating the immunofluorescence of GnRH in various DEHP treatment groups and control groups ($n = 6$, Student's t test, $^{***}p < 0.001$). **D** Bar chart displaying the alterations in GnRH, FSH, estradiol, and progesterone protein levels in the serum of different treatment groups and control groups ($n = 6$, Student's t test, $^{**}p < 0.01$; $^{***}p < 0.001$).

statistically significant difference was observed in DEHP residues among different organs after long-term DEHP exposure compared to the short-term group, higher residues of DEHP were observed in these tissues of long-term treated mice. These results suggest that the disruptive effects of DEHP may not only stem from its direct influence on the gut but also extend to other critical organs, such as the brain, by crossing the blood-brain barrier through systemic circulation.

DEHP deteriorates ovarian function and fertility in mice

Exposure to DEHP slightly reduced body weights in mice over the 32-day exposure period, however no significant differences were detected when compared to control group (Fig. 1B). Both the short-term and long-term exposure to DEHP reduced the pregnancy rates and litter sizes of mice (Fig. 1C, D), in particular the short-term DEHP exposure led to a significant decrease in the number of fetuses with a value of 38.20 ± 8.10% when compared to control group (Mann–Whitney U test, $p < 0.01$; Fig. 1D). Histological analysis of ovarian tissues obtained from mice exposed to DEHP revealed noticeable disparities in follicular morphology. Both the short-term and long-term exposure to DEHP could led to the loosening detachment of granulosa cell structures, wider intercellular gaps between granulosa cells and follicular membranes, and the presence of atretic follicles. Follicle counting indicated that the number of atretic follicles in the ovaries of long-term DEHP-treated mice was significantly increased, while a significantly lower number of antral follicles were both observed in short-term and long-term DEHP treatment (Fig. 1E). These findings collectively demonstrate that both short-term and long-term exposure to DEHP induce an obvious reproductive toxicity in female subjects, despite DEHP did not show significant effects on body weight in mice.

DEHP exposure disturbed the secretion of hypothalamic-pituitary-ovarian axis-related hormones

Both the immunofluorescence (Fig. 2A) and immunohistochemical (Fig. 2B) analyses clearly showed the significant effects of DEHP exposure on the GnRH expression within the hypothalamic arcuate nucleus. Specifically, exposure to DEHP significantly increased the expression of GnRH in mice when compared to control group, with the values of 150.7 ± 5.2% (Student's t test, $p < 0.001$) and 199.9 ± 7.1% (Student's t test, $p < 0.001$) in the short-term and long-term periods treatments, respectively (Fig. 2C).

Meanwhile, we used an ELISA method to examine the HPO axis-mediated reproduction-related hormone indicators in the blood of

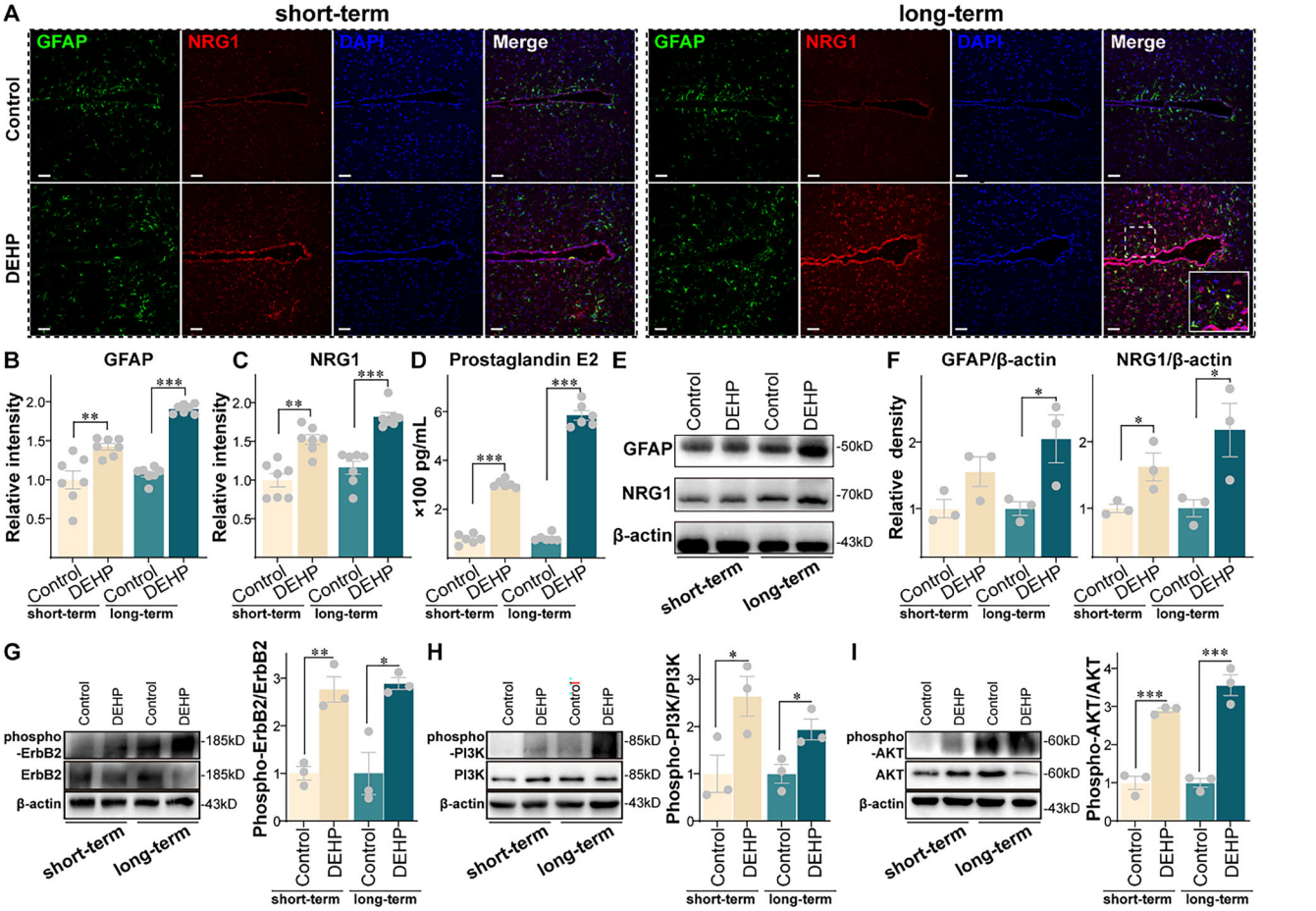

Fig. 3 | DEHP interference with astrocytes in the arcuate nucleus of the hypothalamus and potential mechanisms underlying the increase in GnRH release by DEHP. A–C Representative graphs and statistical plots illustrating the immunofluorescence of GFAP ($n = 6$, Student's t test, $^{**}p < 0.01$, $^{***}p < 0.001$) and NRG1 ($n = 6$, short-term exposure group: Mann–Whitney U test, $^{**}p < 0.01$; long-term exposure group: Student's t test, $^{***}p < 0.001$) in various DEHP treatment groups and control groups. Scale bars: 50 μm. **D** Bar chart displaying the changes in Prostaglandin E2 (PGE2) protein levels in the serum of different treatment groups ($n = 6$, Student's t test, $^{***}p < 0.001$). **E, F** Representative immunoblot and quantification showing changes in GFAP/β-actin and NRG1/β-actin in different DEHP treatment groups compared to controls. ($n = 3$, Student's t test, $^{*}p < 0.05$). **G–I** Representative immunoblot and quantification showing changes in phosphor-ErbB2/ErbB2, phosphor-PI3K/PI3K and phosphor-AKT/AKT in different DEHP treatment groups compared to controls. ($n = 3$, Student's t test, $^{*}p < 0.05$; $^{**}p < 0.01$; $^{***}p < 0.001$).

mice exposed to DEHP in the short-term and long-term periods (Fig. 2D). We found that both the short-term and long-term DEHP exposure significantly increased the serum levels of GnRH and FSH in mice as compared to control group (Student's t test, $p < 0.001$). Specifically, the GnRH and FSH levels were 669.6 ± 23.71 pg/mL and 31.8 ± 1.2 ng/mL in the short-term DEHP exposure treatment, while further increased to the levels of 835.3 ± 16.5 pg/mL and 60.4 ± 4.6 ng/mL in the long-term DEHP exposure treatment. In contrast, estradiol and progesterone levels showed completely opposite trends in the long-term and short-term DEHP exposure treatments. In a short-term experiment, DEHP exposure significantly upregulated the estradiol and progesterone hormones levels as compared to control group (Student's t test, $p < 0.01$). However, lower levels of estradiol and progesterone hormones were observed in the long-term DEHP exposure treatment as compared to control group (Student's t test, $p < 0.001$).

Furthermore, linear regression analysis results showed that the levels of GnRH ($p < 0.001$), FSH ($p < 0.001$), estradiol ($p = 0.02$), and progesterone ($p = 0.10$) hormones were all negatively correlated with the pregnancy rate in mice (Supplementary Fig. 2A). These findings suggest that the DEHP exposure may deteriorate the fertility in mice by disrupting the regulatory homeostasis of reproduction-related hormones within the HPO axis.

DEHP induced activation of mouse hypothalamic astrocytes and upregulation of NRG1 expression

Immunofluorescence staining of GFAP and NRG1 was used to evaluate the effects of DEHP on astrocyte activation and NRG1 expression. We noticed that both the short-term and long-term DEHP exposure could activate astrocytes in the hypothalamic arcuate nucleus region (Fig. 3A), which resulted in a significant increase in the expression of GFAP (accounted for 142.1 ± 4.2% of short-term Control, and 176.3 ± 2.3% of long-term Control, Fig. 3B) and NRG1 (accounted for 152.3 ± 6.3% of short-term Control, and 155.1 ± 5.5% of long-term Control, Fig. 3C), as compared to the control group (GFAP: Student's t test, $p < 0.01$; Mann–Whitney U test for the long-term DEHP treatment group, $p < 0.001$, Student's t test for the short-term DEHP treatment group, $p < 0.01$). In particular, these influences of DEHP were furtherly found to be accompanied by changes in the serum hormones levels of prostaglandin E2 (PGE2). Results showed that the DEHP exposure significantly increased the levels of serum PGE2 both in the short-term and long-term experiments as compared to Control group, with values of 303.9 ± 6.5 pg/mL (Student's t test, $p < 0.001$) and 584.7 ± 19.7 pg/mL (Student's t test, $p < 0.001$), respectively (Fig. 3D).

Observed findings in the immunofluorescence staining experiments were furtherly corroborated by the hypothalamic protein extraction experiment and western blot analysis. Specifically, significantly higher relative densities of GFAP/β-actin (accounted for 155.8 ± 14.9% of short-

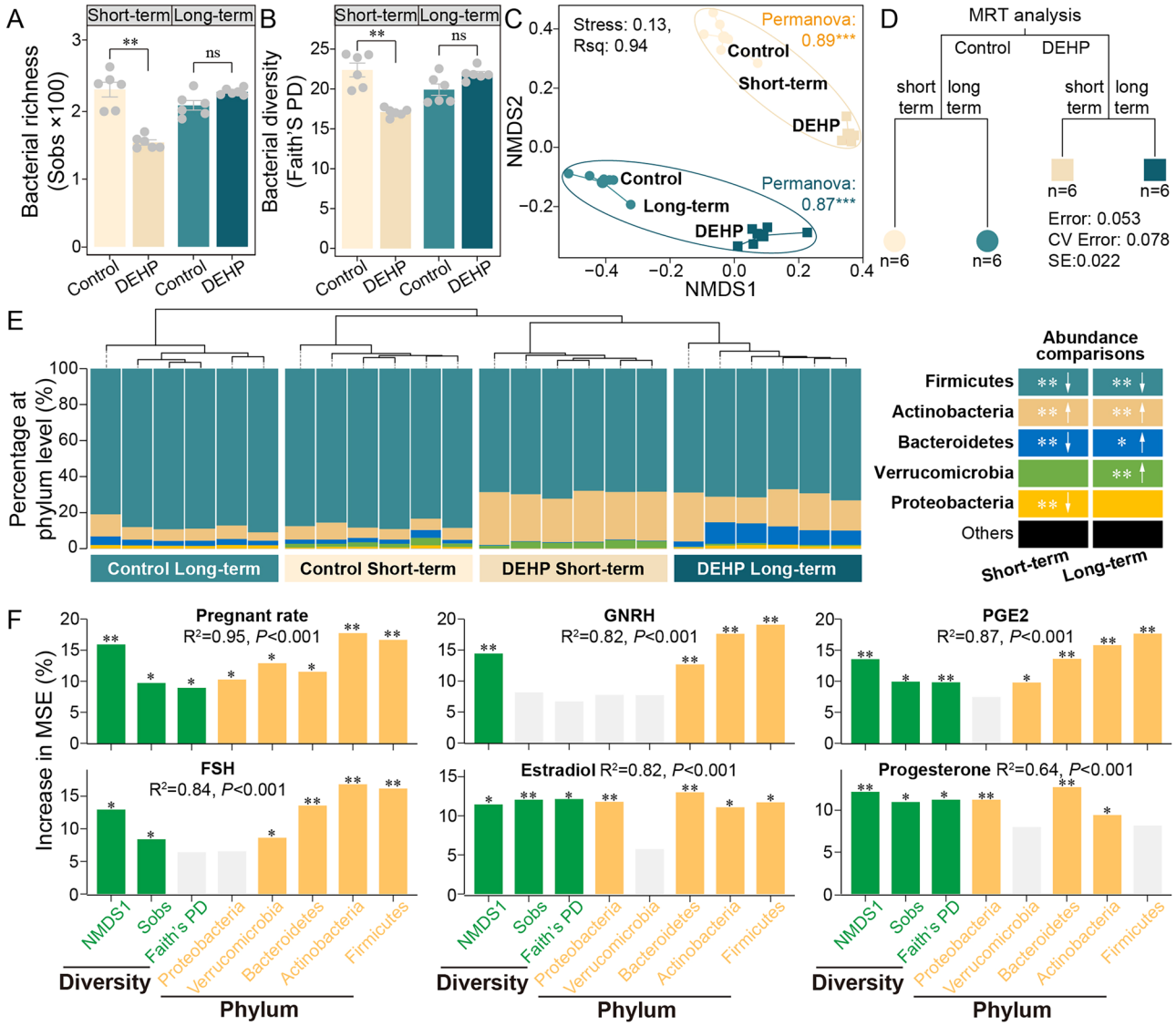

Fig. 4 | Variation patterns of intestinal microbial diversity and community composition in short-term and long-term DEHP exposure periods. A Bacterial richness (Sobs) and **B** bacterial diversity (Faith's PD) among all treatments ($n = 6$, mean ± SE). **C** Non-metric multidimensional scaling (NMDS) ordinations analysis of bacterial community composition across all treatments. Differences in bacterial community composition (NMDS) of different treatments were determined by analysis of permutational multivariate analysis of variance (PERMANOVA; $^{***}p < 0.001$). **D** Multiple regression tree (MRT) analysis of effects of DEHP treatment and treated time on bacterial community composition. The R^2, error, cross-validation error (CV Error), and standard error (SE) of MRT analysis were listed under the tree. **E** Percent stacked bar chart based on the relative abundances of bacterial phyla, showing hierarchical clustering along with DEHP treated and control groups on top of the graph. Color blocks on the right show phyla names, the key on the right show significant changes and their direction (upward and downward arrows for increased and reduced abundances, respectively) for each phylum as compared DEHP treatment with control group, in short-term and long-term respectively (Student's t test, $^{*}p < 0.05$; $^{**}p < 0.01$). **F** Random Forest (RF) mean predictor importance (percentage of increase of mean square error (MSE), increase in MSE%) of bacterial diversity indices (NMDS1, sobs and Faith'S PD) and phyla abundances as drivers for mouse pregnancy rate and levels of HPO axis-related hormones comprised of Follicle-Stimulating Hormone (FSH), GnRH, Estradiol, PGE2 and Progesterone. The accuracy importance measure was computed for each tree and averaged over the forest (5000 trees). Percentage increases in the MSE of variables were used to estimate the importance of these predictors, and higher MSE% values imply more important predictors. Significance levels are as follows: $^{*}p < 0.05$; $^{**}p < 0.01$.

term Control, and 205.1 ± 25.4% of long-term Control; Student's t test, $p < 0.05$) and NRG1/β-actin (accounted for 162.2 ± 12.6% of short-term Control, and 217.9 ± 27.7% of long-term Control; Student's t test, $p < 0.05$) can be found both in the short-term and long-term DEHP exposure groups (Fig. 3E, F). Furthermore, we found the levels of serum PGE2 showed a significant negative relationship with pregnant rate ($p < 0.001$, Supplementary Fig. 2B), which were significantly positively correlated with the relative densities of GFAP and NRG1 ($p < 0.001$, Supplementary Fig. 2C). These results suggest a potential association between astrocyte activation, NRG1 release, and PGE2 release induced by DEHP exposure.

DEHP exposure impacted the proteins related to the ErbB2-PI3K/AKT pathway in mouse hypothalamus

Western blot analysis revealed that both the short-term and long-term DEHP exposure significantly elevated the levels of phosphorylated ErbB2 (p-ErbB2), phosphorylated PI3K (p-PI3K), and phosphorylated AKT (p-AKT) proteins in the hypothalamus of mice as compared to control groups (Student's t test, $p < 0.05$; Fig. 3G–I). Specifically, in the DEHP treatment group, the ratio of p-ErbB2 and ErbB2 accounted for 276.2 ± 6.1% of short-term Control, and 288.5 ± 19.8% of long-term Control (Fig. 3G); the ratio of p-PI3K and PI3K accounted for 264.1 ± 10.8% of short-term Control, and 193.8 ± 18.1% of long-term Control (Fig. 3H); the ratio of p-AKT and AKT

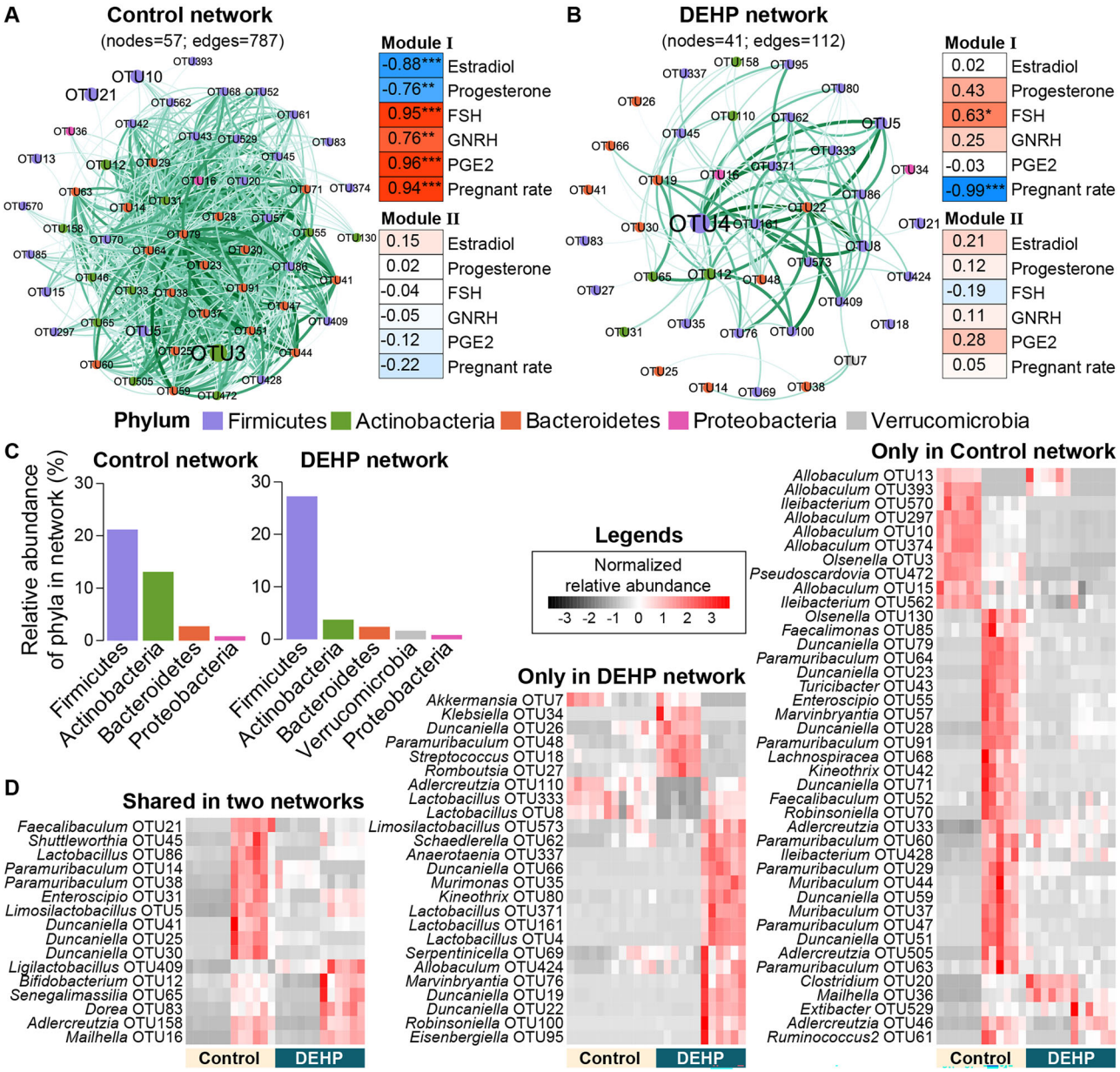

Fig. 5 | Bacterial OTU co-occurrence network and module-trait associations. Co-occurrence networks of Control group (**A**) and DEHP treatment (**B**) with OTU (nodes) colored according to the phyla to which they belong. Any resulting correlations with p value ≥ 0.01 and abs(r) <0.3 were removed. Green lines with different thicknesses were drawn by the weight of the edges. Module-trait associations between one OTU module with a HPO axis-related hormones trait or mouse pregnant rate are shown by color blocks (red for positive correlations and blue for negative correlations) which contain the correlation and the corresponding p value (*$p < 0.05$; **$p < 0.01$; ***$p < 0.001$). **C** Cumulative relative abundances of phyla in Control and DEHP networks. **D** Heatmaps showing the normalized relative abundances of shared and unique bacterial OTUs between Control and DEHP networks.

accounted for 290.4 ± 1.3% of short-term Control, and 356.1 ± 17.8% of long-term Control (Fig. 3I), respectively. These findings suggest that DEHP exposure may induce PGE2 release through astrocyte activation, which is mediated by the ErbB2-PI3K/AKT signaling pathway.

DEHP exposure shifted the diversity and composition of intestinal microbiome

Intestinal contents sampled from the short-term and long-term treatment groups were both used to examine whether DEHP exposure shifted the diversity and composition of intestinal microbiome. Significant lower bacterial richness index (sobs) and diversity index (Faith's PD) were observed in the DEHP short-term treatment group as compared to the short-term control group (Student's t test, $p < 0.01$, Fig. 4A, B). However, these *alpha* diversity indices did not differ significantly between the DEHP and control groups in the long-term treatment.

We conducted non-metric multidimensional scaling (NMDS) analysis and Multiple regression tree (MRT) analyses to visualize the differences in the intestinal microbiome and identify treatment factors associated with patterns of bacterial community composition, respectively. NMDS results clearly showed significant differences in bacterial community composition between DEHP and control groups both in the short-term (PERMANOVA test, $R^2 = 0.89$, $p < 0.001$) and long-term (PERMANOVA test, $R^2 = 0.87$, $p < 0.001$) treated periods (Fig. 4C). Overall, bacterial community composition from short-term treatment groups was distinctly separated from long-term treatment groups along the second component (NMDS2). Bacterial community composition from DEHP treatment was distinctly separated

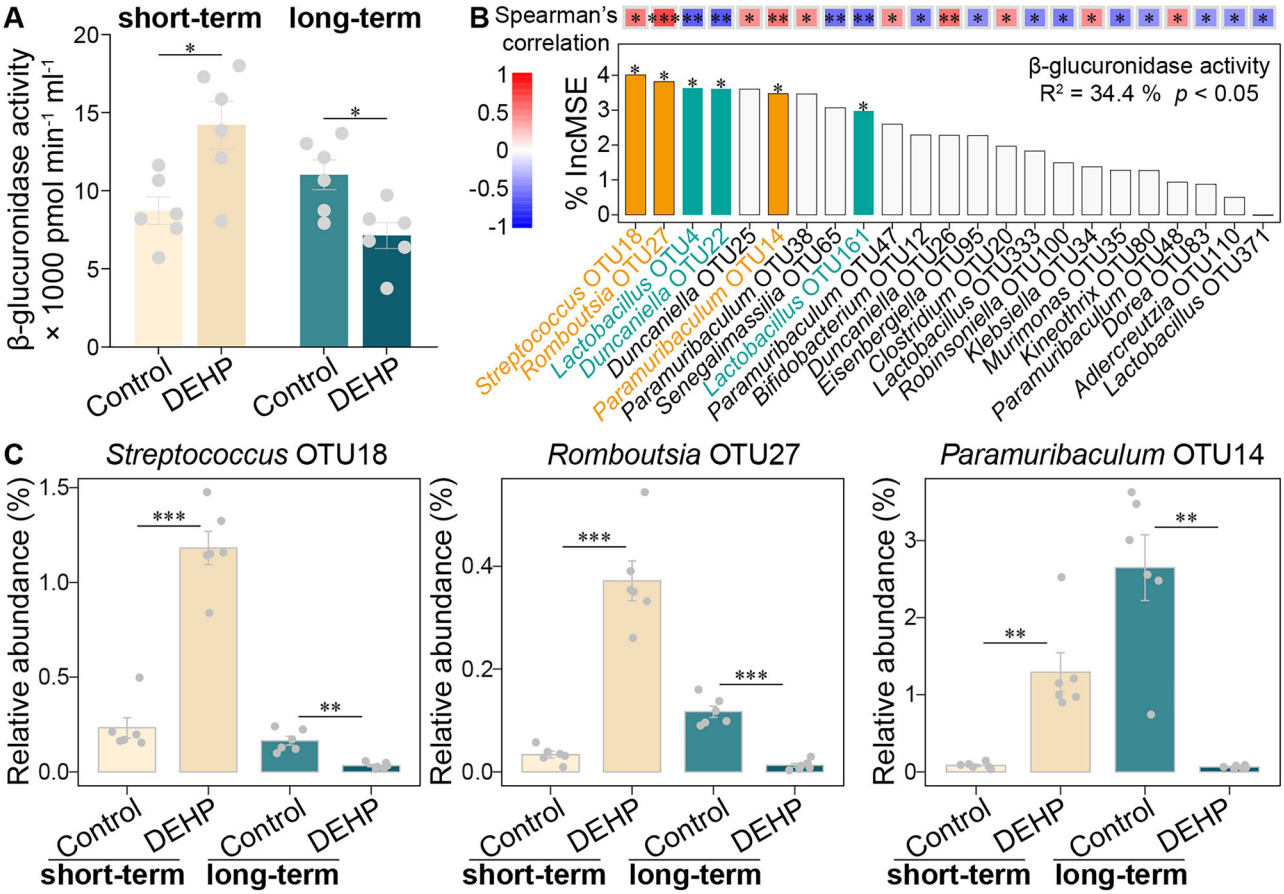

Fig. 6 | The gut microbiota relationships with Estrogen. A Bar chart displaying the alterations in GUS enzyme activity in the intestinal contents of DEHP treatment and Control groups ($n = 6$, Student's t test, $^*p < 0.05$). **B** Random Forest (RF) mean predictor importance (percentage of increase of mean square error (MSE), increase in MSE%) of bacterial OTUs as drivers for GUS enzyme activity. The accuracy importance measure was computed for each tree and averaged over the forest (5000 trees). Percentage increases in the MSE of variables were used to estimate the importance of these predictors, and higher MSE% values imply more important predictors. Significance levels are as follows: $^*p < 0.05$. Color blocks with asterisks represent Spearman's correlations between bacterial OTUs and GUS enzyme activity ($^*p < 0.05$; $^{**}p < 0.01$; $^{***}p < 0.001$). **C** The relative abundances of GUS-related gut bacteria among all treatments (Student's t test, $^{**}p < 0.01$; $^{***}p < 0.001$).

from control along the first (NMDS1) and the second (NMDS2) component, both in the short-term and long-term treated periods. Notably, these observations were supported by multiple regression tree (MRT) analysis which showed that bacterial communities could be split into two major groups according to whether or not they had been treated by DEHP, with a further separation of short-term and long-term treated periods (Fig. 4D). PERMANOVA test also confirmed the significant effects of DEHP treatment (PERMANOVA test, $R^2 = 0.34$, $p < 0.001$) and treated time (PERMANOVA test, $R^2 = 0.38$, $p < 0.001$).

Bacterial community composition differences between DEHP treatment with control were found to be accompanied by significant changes in the relative abundances of different bacterial phyla (Fig. 4E). Short-term exposure to DEHP significantly decreased the relative abundances of Firmicutes, Bacteroidetes and Proteobacteria, along with the significant enrichment of Actinobacteria density (Student's t test, $p < 0.05$). Long-term exposure to DEHP significantly decreased Firmicutes relative abundance, while significantly enrich the relative abundances of Actinobacteria, Bacteroidetes and Verrucomicrobia (Student's t test, $p < 0.05$).

Potential gut microbial drivers that affecting HPO axis-related hormone and pregnancy rate

To disentangle the potential biological drivers that may affect pregnancy and HPO axis, we identified the main gut bacterial predictors for mouse pregnant rate and HPO axis-related hormone by random forest (RF) analysis (Fig. 4F). Results showed the potential associations between bacterial diversity indices and phyla densities variations in gut with mouse pregnant rate and HPO axis-related hormone level ($p < 0.001$). Among bacterial diversity indices, beta-diversity index (NMDS1, $p < 0.01$) was found to be the most pivotal variable for predicting the mouse pregnant rate followed by alpha-diversity indices (sobs and Faith'S PD, $p < 0.05$). With regard to bacterial phyla, Actinobacteria ($p < 0.01$) were the most pivotal variable for predicting mouse pregnant rate followed by Firmicutes, Verrucomicrobia, Bacteroidetes, and Proteobacteria ($p < 0.05$).

We also showed the potential contributions of bacterial diversity indices and phyla densities variations in affecting HPO axis-related hormones levels (Fig. 4F). Beta-diversity index (NMDS1), alpha diversity index (sobs), the densities variations of Actinobacteria, Firmicutes, Bacteroidetes and Verrucomicrobia were observed as the important variable for predicting FSH level ($p < 0.05$). Beta-diversity index (NMDS1), the densities variations of Firmicutes, Actinobacteria and Bacteroidetes were observed as the important variable for predicting GnRH level ($p < 0.01$). Beta-diversity index (NMDS1), alpha diversity index (sobs and Faith'S PD), the densities variations of Bacteroidetes, Proteobacteria, Firmicutes and Actinobacteria were observed as the important variable for predicting Estradiol level ($p < 0.05$). Beta-diversity index (NMDS1), alpha diversity index (sobs and Faith'S PD), the densities variations of Firmicutes, Actinobacteria, Bacteroidetes and Verrucomicrobia were observed as the important variable for predicting PGE2 level ($p < 0.05$). Beta-diversity index (NMDS1), alpha diversity index (sobs and Faith'S PD), the densities variations of Bacteroidetes, Proteobacteria and Actinobacteria were observed as the important variable for predicting Progesterone level ($p < 0.05$).

Bacterial OTU co-occurrence network and HPO axis associations

To ravel out the diverse functional relationships of microorganisms in the complex intestinal system, we first constructed a co-occurrence network of bacterial operational taxonomic units (OTUs) (Fig. 5A, B). 57 bacterial OTUs identified from four phyla (Firmicutes, Actinobacteria, Bacteroidetes, and Verrucomicrobia) that formed 787 strong links (weighted >0.5) were observed in the control group network (Fig. 5A), while only 112 strongly links (weighted >0.5) formed by 41 bacterial OTUs from five phyla (Firmicutes, Actinobacteria, Bacteroidetes, Verrucomicrobia, and Proteobacteria) were shown in the DEHP network (Fig. 5B).

We then deconstructed these two bacterial networks into smaller coherent modules by using a method that imitating weighted gene co-expression network analysis (WGCNA) to examine potential relationships between bacterial network modules with HPO axis-related hormones and mouse pregnant rate (Fig. 5A, B). Both bacterial networks were all deconstructed into two modules, evidently, not all bacterial modules showed alike and strong relationships with the various HPO axis-related hormones variables and mouse pregnant rate. In the control network, the bacterial module I was significantly and positively correlated with mouse pregnant rate and the levels of HPO axis-related hormones comprised of FSH, GnRH, and PGE2, while significant negative correlations between this bacterial module and Estradiol and Progesterone were observed ($p < 0.01$, Fig. 5A). With regards to DEHP network, only the levels of HPO axis-related hormones FSH and mouse pregnant rate showed significant positive and negative relationships with bacterial module I, respectively ($p < 0.05$, Fig. 5B).

In order to detect the specific bacterial species with remarkable role in affecting HPO axis-related hormones and mouse pregnant, we investigated the variation features in the relative abundances of bacterial OTUs appeared in control and DEHP networks (Fig. 5C, D). Bacterial network nodes were both dominated by species identified from Firmicutes, followed by Actinobacteria, Bacteroidetes, Verrucomicrobia, and Proteobacteria (Fig. 5C). In total, only 16 bacterial OTUs were shared between these two networks, while 41 (72%) and 25 (61%) bacterial OTUs were unique in the Control network and DEHP network, respectively (Fig. 5D). The normalized relative abundances of all bacterial species were also shown in Fig. 5D.

The gut microbiota relationships with Estrogen

Estrogen undergoes glucuronidation for inactivation and transport to the intestine for excretion. Within the intestinal lumen, these estrogen-glucuronide conjugates can be reactivated by β-glucuronidase (GUS) enzymes produced by certain bacteria, thus releasing active estrogen and facilitating enterohepatic recirculation[29]. We observed that GUS enzyme activity in the intestinal contents showed significant variation according to the duration of DEHP exposure (Student's t test, $p < 0.05$; Fig. 6A). We further assessed the associations of key gut microbes in networks with GUS enzyme activity in intestinal contents by using random forest (Fig. 6). *Streptococcus* OTU18 was found to be the most pivotal variable for predicting the GUS enzyme activity in intestinal contents followed by *Romboutsia* OTU27, *Lactobacillus* OTU4, *Duncaniella* OTU22, *Paramuribaculum* OTU14, *Lactobacillus* OTU161 ($p < 0.05$; Fig. 6B). Among the identified OTUs, three key microbes exhibited parallel changes with both estrogen levels and GUS enzyme activity in response to DEHP exposure (Spearman's correlation analysis, $p < 0.05$; Fig. 6B). These GUS-related bacteria were *Streptococcus* OTU18, *Romboutsia* OTU27, and *Paramuribaculum* OTU14 (Student's t test, $p < 0.01$; Fig. 6C).

Discussion

Here, we showed the progressive impacts of DEHP (a commonly used plasticizer) exposure both in short-term and long-term periods on the development of mouse pregnancy and related HPO axis and intestinal microbiome. We reported that the DEHP exposure had a remarkable detrimental impact on mouse litter size by disrupting the homeostasis of HPO axis and intestinal microbiome. Within HPO axis, DEHP abnormally elevated prostaglandin E2 (PGE2) and gonadotropin-releasing hormone (GnRH) by activating hypothalamic astrocytes and increasing neuregulin 1 (NRG1) expression, which are the key regulators of reproductive function. We also present evidence showing the intestinal β-glucuronidase level as well GUS-related microbial taxa densities variation trends, were closely related to disordered changes in estrogen levels, which demonstrate that these adverse effects on pregnancy-related HPO axis can be mediated by specific intestinal microbiota. These studies reveal a mechanism by which HPO axis-related hormones and intestinal microbiome induced by environmental pollutants of DEHP damage mouse fertility.

Hypothalamic-pituitary-ovarian (HPO) axis plays a vital role in safeguarding mammalian reproduction processes by regulating ovulatory function[30] and reproductive hormones secretion[31]. HPO-related endocrine homeostasis is essential for pregnant women and their offspring[32,33], while it is constantly threatened by EDCs present in the environment[34,35]. Similarly, we noticed that the ovarian functions of mouse were distinctly decreased under the DEHP (a typical endocrine disruptor) conditions, which may be related to disruption for the cell cycle of ovarian granulosa cells and oocytes[36,37]. Studies also reported that DEHP exposure can be not only associated with altered ovarian function in women but also can increase miscarriage rates during pregnancy and even reduce reproductive capacity in their offspring[38–41], and our observation of lower litter size in DEHP treatment support these findings. We also showed strong links between the altered HPO axis-related hormones with mouse pregnancy. DEHP short-term treated significantly increased the secretion levels of HPO axis-related hormones comprised of FSH, GNRH, Estradiol, PGE2 and Progesterone, which was associated with lower mouse pregnancy rate. These findings are in accordance with previous studies, which reported that DEHP can interfere with the secretion of reproductive hormones such as estrogen and testosterone in both mothers and their offspring[8,42]. Furthermore, we noticed that with prolonged exposure to DEHP, the secretion of GnRH, PGE2, and FSH continues to increase, while estradiol and progesterone secretion levels display an obvious decreasing trend instead. This discrepancy may be attributed to ovarian damage caused by prolonged DEHP exposure[36], which ultimately leads to reduced secretion of estradiol and progesterone. Indeed, our findings demonstrated that DEHP exposure can disrupt the function of HPO axis, and thereby affecting the mouse pregnancy rate.

Our study found disorder release of GnRH may be mediated by activation of astrocytes in hypothalamus. Astrocytes are the mediators of intermittent hormone release among Gonadotropin-releasing hormone (GNRH) neurons[43,44], which play an important role in modulating neuroendocrine function[45,46]. It has been reported that astrocytes could interact with GNRH neurons present in the hypothalamic arcuate nucleus (ARC) by releasing glial transmitters PGE2[47,48] which could enhance GNRH neuronal activity and stimulate GnRH release[49]. The observation of higher levels of PGE2 and GnRH in DEHP treatment supports these findings and expand upon prior investigations, which indicating that the DEHP can stimulate the release of PGE2 by activating astrocytes in the hypothalamus and thereby regulating the release of GNRH in GNRH neurons. Notably, our study can demonstrate that DEHP exposure was capable of activating astrocytes and promoting the secretion of NRG1 within hypothalamus, which was associated with higher level of PGE2 in DEHP mouse astrocytes[22,50,51]. Previous studies reported that the NRG1 exerts its biological effects within hypothalamic astrocytes by interacting with ErbB receptors[50], initiating intracellular signaling cascades involving second messengers, including the PI3K-AKT pathway[52,53]. We also found that both short- and long-term DEHP exposure activates the ErbB2-PI3K/AKT signaling pathway, enhancing PGE2 release and disrupting hormonal balance.

Gut microbiome as human second genome can communicate with various organs by the gut-organ axis[11], and any changes in intestinal microbial composition can be linked to both the basic physiological functions and the occurrence of diseases[54,55]. We also found remarkable links between DEHP-induced intestinal bacterial community with HPO axis-related hormones levels, ovarian function and fertility. Several previous

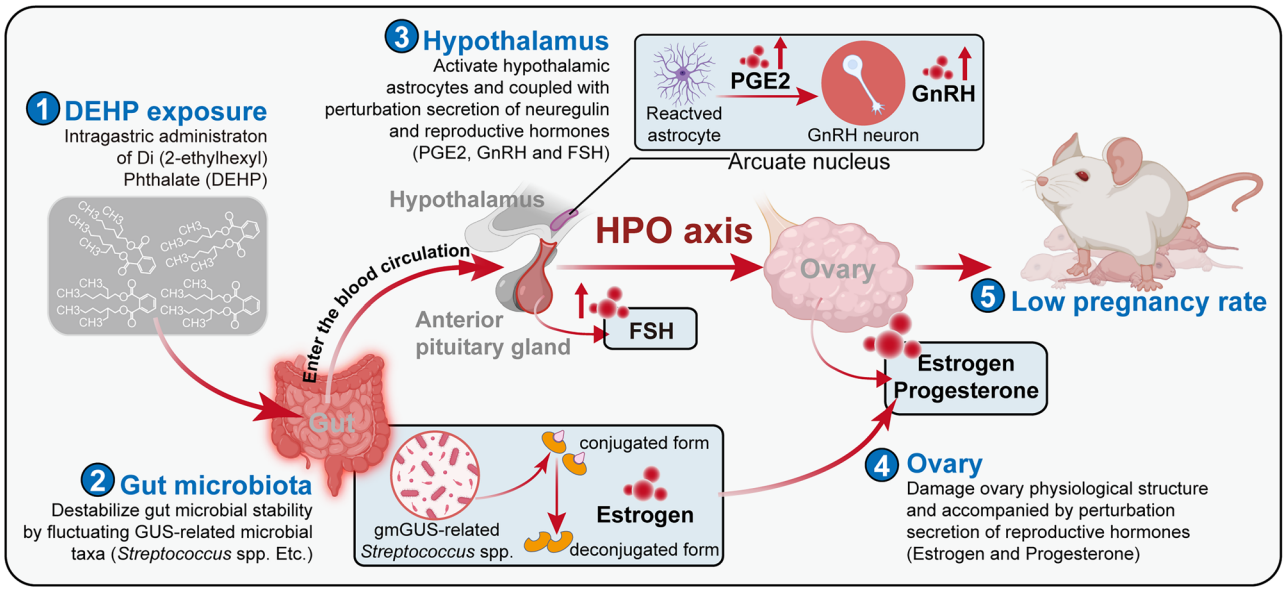

Fig. 7 | Conceptual model illustrating the proposed sequence of events taking place in gut, hypothalamus and ovary of female rats intragastric administration with DEHP. Depicted are the DEHP exposure can (1) activate hypothalamic astrocytes and coupled with perturbation secretion of neuregulin and reproductive hormones (PGE2, GnRH and FSH); (2) destabilize gut microbial stability by fluctuating GUS-related microbial taxa (*Streptococcus* spp. Etc.) that accompanied by perturbation secretion of reproductive hormones (Estrogen); (3) damage ovary physiological structure and accompanied by perturbation secretion of reproductive hormones (Estrogen and Progesterone), and thereby disrupting the microbe-gut-hypothalamic-pituitary-ovarian axis (MGHPO) that cause a decrease of pregnancy rate in mice. Diagram was created using BioRender.

studies have reported that lower intestinal bacterial diversity in environmental pollutants treated mouse related to fertility[16,56], and our observation of lower indices in bacterial Sobs and Faith's PD in DEHP treatment supported these findings. Similar patterns also shown in comparisons of healthy versus ovarian-related diseases women, and higher bacterial diversity was always found in gut of healthy groups[57]. Our data also showed clear shifts in specific bacterial compositions induced by DEHP, in which abundances variation of Firmicutes, Proteobacteria, and Actinobacteria were significantly contributed to HPO axis-related hormones and mouse pregnancy rate both in random forest and linear regression analyses. These findings are in accordance with previous studies, which reported that endocrine disruptor exposure could affect reproductive-related physiological functions, such as ovary functions and related hormones, by disturbing the intestinal microbial compositions[16,56]. Notably, these observed shifts in intestinal bacterial compositions and their potential functions were also reflected in their network construction patterns. DEHP network showing fewer nodes and links, which weaken link strength between specific network modules to HPO axis-related hormones levels and mouse pregnancy rate. Several previous studies have reported that more complicated network interactions in microbial community are more conducive to stable implementation of physiological function[58,59], and our observation of decreased ovarian function and lower mouse pregnancy rate in DEHP treatment supports these findings. These results demonstrated that the homeostasis of gut microbiome have strongly related to the reproductive functions of mice.

Notably, we showed shifts in bacterial community induced by DEHP were closely reflected in the activity of gut β-glucuronidase (GUS) enzyme, which is related to estrogen regulation[60]. We found variations in GUS were consistent with changes in estrogen levels, suggesting that DEHP-manipulated gut microbiota can express specific enzymes to regulate HPO-related hormone secretion[29]. Moreover, we were able to identify several candidate driver taxa that played a key role in bacterial co-occurrence networks and were changed paralleled the alterations in estrogen levels and GUS enzyme activity following DEHP exposure. For example, *Staphylococcus* genera, which has previously been shown to have high GUS enzyme production activity specifically for estrogen reactivation[61,62], indicating its involvement in modulating estrogen homeostasis within HPO axis. While direct action mechanism of *Romboutsia* and *Paramuribaculum* on estrogen is less well understood, previous studies have reported that DEHP exposure can significantly shift *Romboutsia* abundance that related to alteration of estrogen levels[16,63], which may by its role in lipid metabolism[64]. These findings suggest that adverse effects of DEHP on HPO axis may be further reinforced by specific bacterial taxa in intestinal microbiome, which can produce functional enzymes and influence hormone secretion. Indeed, we demonstrated that DEHP can decrease pregnancy rate of mice by disrupting the intestinal microbiome-driven HPO axis homeostasis. In the future, it would be interesting to use these taxa to study the relationships and molecular mechanisms between microbe gut-HPO axis and pregnancy.

Genetic inheritance and external environmental factors jointly determine the development and health of human[65–67]. Despite numerous studies have found that some specific environmental factors can be the triggers for many genetic and non-genetic diseases[68,69], mechanisms are still relatively poorly understood given the complexity of environment-human interactions and the dependence of these interactions on environmental conditions[70,71]. The current study clearly demonstrated that DEHP could persist in the gut-HPO axis and disturb the homeostasis of gut microbiome-driven HPO-related hormones. Notably, after DEHP exposure, loss of intestinal microbial network stability, fluctuation of β-glucuronidase activity-related microbial taxa (*Streptococcus* spp. Etc.) abundances in gut, and activation of hypothalamic astrocytes coupled with perturbation secretion of neuregulin and reproductive function-related hormones play crucial roles in this process (Fig. 7). These findings obtained herein suggest a novel mechanism for elucidating the fertility toxicity effects of DEHP and stress the importance of biosafety evaluation of plasticizers to ensure accurate risk assessment of plastic pollutants.

Methods

Preparation of DEHP for treatment and concentrations

DEHP was obtained from Sigma-Aldrich (USA). In the control groups, corn oil (1 mL/kg) was administered orally on a daily basis, while in the DEHP groups, a dose of 300 mg/kg/day of DEHP dissolved in 1 mL/kg corn oil was administered orally, as described by Li et al.[72]. The short-term groups

received treatment for 16 days, while the long-term groups received treatment for 32 days.

Animal maintenance and treatment

Male and female C57BL/6J mice with specific pathogen-free (SPF) status, aged 8 weeks, were acquired from the Experimental Animal Center of Nanjing Medical University. The mice were housed in a controlled environment (temperature: 22 °C, light/dark cycle: 12 h) and subjected to a 1-week acclimatization period. All procedures were approved by the Institutional Animal Care Committee of Nanjing Medical University in alignment with the Chinese Council on Animal Care guidelines. Female mice were randomly assigned to four groups ($n = 20$ per group): short-term control, short-term DEHP, long-term control, and long-term DEHP.

Experimental group setup and mating procedure

On the 16th or 32nd day of the treatment period, 80 female mice were then cohabitated with 40 male mice for 3 days, with the first day of cohabitation designated as day 1. On day 18, all cohabitated female mice were sacrificed to examine pregnancy status via cesarean section.

Blood collection

Mice were first anesthetized with isoflurane, placed in a secure restraint, and 100 μL of blood was collected using a 100 μL capillary tube (Microhematocrit Tube, Nonheparinized, Jorgensen Laboratories, Loveland, CO) from the retroorbital sinus of the right eye exclusively, ensuring minimal injury to surrounding tissues.

Tissue collection and preservation

Concurrent with the above procedures, the remaining 80 mice (non-mated) were sacrificed on the 16th or 32nd day between 08:00 a.m. and 11:00 a.m. All mice were euthanized under CO_2 anesthesia, and every effort was made to minimize their suffering and distress throughout the experimental procedures (Supplementary Fig. 1). Brain tissues were immediately excised and preserved in 4% paraformaldehyde solution. Hypothalamus and intestinal contents were collected and rapidly frozen in liquid nitrogen for further analyses.

DEHP residue quantification in tissues

Utilizing high-performance liquid chromatography-tandem mass spectrometry (HPLC–MS/MS), quantification of DEHP residues within prominent murine organs and tissues was conducted subsequent to exposure. The sample underwent homogenization and subsequent sonication on ice. Acetonitrile (Sigma, Saint Louis, USA) was added, followed by centrifugation. The above extraction steps were repeated for secondary extraction. The two supernatants were combined, and preliminary sample preparation was completed by adding acetone (Sigma, Saint Louis, USA), sodium chloride (Sigma, Saint Louis, USA), and anhydrous sodium sulfate (Sigma, Saint Louis, USA) prior to centrifugation. Subsequently, the samples underwent solid-phase extraction column filtration, followed by 0.22 μm organic filter filtration for analytical determination. Refer to previous studies for specific methods[73].

Western blotting analysis

The murine hypothalamic tissue was subjected to homogenization in ice-cold RIPA lysis buffer, fortified with a comprehensive EDTA-free protease inhibitor mixture and PhosSTOP Phosphatase Inhibitor. The homogenate experienced six cycles of sonication lasting 4 s each, with 6-s intervals on ice, followed by centrifugation at 12,000 × g for 20 min at 4 °C. Subsequent to supernatant collection, protein concentration was gauged through the BCA assay. Equal protein quantities were resolved via sodium dodecyl sulfate-polyacrylamide gel electrophoresis (SDS-PAGE) and then transferred onto polyvinylidene difluoride (PVDF) membranes. Following a room temperature blockage of the membrane with 5% BSA for 1-h, overnight incubation at 4 °C with primary antibodies ensued. The primary antibodies used in this study included anti-GFAP (CST, 80788), anti-Nrg1 (proteintech, 66492-1-Ig), anti-p-ErbB2 (CST, 2243S), anti-ErbB2 (proteintech,18299-1-AP), anti-p-AKT (CST, 4060), anti-p-Pi3K (CST, 17366), anti-AKT (proteintech, 10176-2-AP), anti-Pi3K (CST, 4257), and β-actin (zenbio, 380624). After washing the membrane three times with TBST, it was incubated with HRP-linked anti-rabbit IgG secondary antibody (proteintech, SA00001-9) or HRP-linked anti-mouse IgG secondary antibody (proteintech, SA00001-8) at room temperature for 1 h. Following three additional washes with TBST, the protein bands were visualized using Clarity™ ECL western blot substrate (tanon, 180-506) and captured using the ChemiDoc Touch imaging system (Bio-Rad).

Immunohistochemistry assay

Brain sections were deparaffinized using xylene (2x) and subsequently rehydrated through a descending series of ethanol solutions. To quench endogenous peroxidase activity, sections underwent a 10-min treatment with 3% H_2O_2. Following this, they were subjected to a 30-min blocking step at 37 °C using 3% BSA. Next, sections were subjected to an overnight incubation at 4 °C with a primary mouse anti-GnRH antibody (proteintech, 26950-1-AP), succeeded by a 1-h incubation at 37 °C with an HRP-conjugated secondary antibody. Detection of specific binding was achieved using the diaminobenzidine (DAB) method, following manufacturer guidelines (Zhongshan Biotechnology, Beijing, China). Ultimately, sections were counterstained with hematoxylin and mounted with neutral balsam for observation under a Nikon DXM12000F microscope (Tokyo, Japan).

Hematoxylin and eosin (H&E) staining and follicle counting

Sections from ovarian tissues of the four experimental groups underwent immunohistochemical analysis. Paraffin sections were dewaxed, followed by heat-mediated antigen retrieval using microwave irradiation in a pH 6.0 10 mM sodium citrate solution for 15 min. After cooling, sections were thrice rinsed with PBS. Procedures adhered to the SP Rabbit & Mouse HRP Kit (DAB) manufacturer's instructions. Primary antibodies (Abs) against 8-hydroxyguanosine (8-OHdG), 4-hydroxynonenal (4-HNE), nitrotyrosine (NTY), and P16 were incubated overnight. Negative control samples were treated with biotin-conjugated goat antibody against rabbit IgG (H + L). Sections were retained with hematoxylin for 30 s. Uniform antibody concentrations and conditions were employed across all sections. Microscopy facilitated observation and imaging. A representative sample of at least three ovaries from each group was selected. The number of antral and atretic follicles was counted from five interval sections, according to previous studies with minor modifications[16].

Immunofluorescence assay and measurement of intensity

Frozen brain sections (hypothalamus) with a thickness of 20 μm were obtained using a cryostat, following the coordinates from Bregma −3.3 to −4.16 mm. The cutting process took place at a temperature of −18 °C. Subsequently, the brain slices were subjected to blocking with 10% goat normal serum for 15 min at room temperature. Following the blocking step, the sections were incubated overnight at 4 °C with the primary antibodies: anti-GFAP (CST, 80788, 1:200), anti-Nrg1 (proteintech, 66492-1-Ig, 1:250), anti-GnRH (proteintech, 26950-1-AP, 1:800), Mouse (G3A1) mAb IgG1 Isotype Control (CST, 5415), and Rabbit (DA1E) mAb IgG1 XP® Isotype Control (CST, 3900). After washing with PBS, the sections were exposed to the secondary antibodies for 1 h at 37 °C. The secondary antibodies used were DAM cy3 (Jackson, 158838) and DAR488 (Jackson, 157934). Finally, the sections were counterstained with DAPI (biofrox, EZ7890A120). The morphology of the hypothalamus was captured using an OLYMPUS IX51 microscope. The imaging of the hypothalamus in the brain tissue sections was performed using a Leica SP8 confocal microscope system (Leica, Germany). The acquired images of the hypothalamus were processed using the LAS X software (Leica, Germany).

All sections being compared were processed in the same immunohistochemical experiment. Fluorescent images were captured with identical exposure time without saturation of pixel intensities. By using ImageJ software, the DAPI signal in the arcuate nucleus was used to determine the

outline of cell bodies. To measure GNRH GFAP, and NRG1 protein intensity, background was determined based on average intensity value in several areas without any detectable GNRH GFAP, and NRG1 immunoreactivity. GNRH GFAP, and NRG1 intensity in the neurons were determined as signals over the background intensity[74].

Measurement of serum cytokines (ELISA) assay

ELISA kits were used to measure GnRH, PGE2, FSH, estradiol and progesterone of serum according to the manufacturer's instructions (Elabscience Biotechnology Co., Ltd). In the ELISA assays, 5 μL of serum was used for GNRH, PGE2, progesterone, and estradiol, while 10 μL of serum was used for FSH. Serum samples were diluted 10-fold with sterile PBS buffer before proceeding with the assays. Importantly, no pooling of samples was performed, and each sample was analyzed individually.

Sample collection and DNA extraction of intestinal contents

Intestinal content samples from the jejunum and ileum were obtained in accordance with established protocols[75] and preserved at −80 °C until DNA extraction. For each of the 24 samples (comprising 2 treatments: DEHP and Control, 6 replicates, and 2 time points: 16 days short-term and 32 days long-term), DNA was extracted from a 0.25 g sample using the PowerSoil DNA Isolation Kit (Mobio Laboratories, Carlsbad, CA, USA), adhering to manufacturer guidelines. DNA concentration and quality were assessed using a NanoDrop 2000 spectrophotometer (Thermo Scientific, Waltham, MA, USA).

16S rRNA gene sequencing for intestinal microbiome

Intestinal bacterial communities were investigated by using the general universal bacterial primers 338 F (5'-ACT CCT ACG GGA GCA GCA G-3') and 806 R (5'-GGA CTA CHV GGG TWT CTA AT-3') to amplify the V3-V4 region of the bacterial 16S rRNA gene from DNA samples[76]. The library construction and sequencing for bacterial communities were carried out on an Illumina MiSeq PE250 platform at Personal Biotechnology Co., Ltd (Shanghai, China), following the standard protocols and instructions. Amplification sequence processing and OTU table generating were performed by using UPARSE pipeline[77]. Briefly, "fastq_mergepairs", "fastq_trunclen", "fastq_filter", "fastx_uniques", and "cluster_otus" commands were used in turn for forward and reverse sequences merging, sequences trimming (300 bp), sequences quality filtering, operational taxonomic units (OTUs) forming, and OTU table file generating. The representative sequence for each OTU was selected and classified using the RDP classifier against the RDP Bacterial 16S database[78].

β-Glucuronidase activity

Using the β-Glucuronidase Activity Assay Kit (Fluorometric) (ab234625), we measured the enzyme activity in the intestinal contents from the jejunum. The assay was performed according to the manufacturer's protocol with minor modifications based on previous methodologies[79]. Briefly, intestinal samples were homogenized and processed to obtain clear lysates, which were then incubated with the assay reagents. Fluorescence intensity, indicating β-glucuronidase activity, was measured at the specified wavelength and normalized against protein concentration to account for sample variability.

Bacterial community diversity and composition profile statistical analysis

Bacterial richness (Sobs) and diversity (Faith's phylogenetic diversity (Faith's PD)) indices were calculated as *Alpha*-diversity and were performed in MOTHUR[80,81]. Non-metric multidimensional scaling (NMDS) based on a Bray-Curtis dissimilarity matrix was performed and plotted to explore the differences in bacterial communities[82]. The method of permutational multivariate analysis of variance (PERMANOVA) was used to determine the significance of differences in bacterial community compositions[82,83]. The impacts of short-term and long-term DEHP treatments on intestinal bacterial communities were evaluated by multiple regression tree (MRT) analysis[84]. Main bacterial predictors (Sobs, Faith's PD, NMDS1, phyla, and selected OTUs) for pregnant rate and fertility-related hormone levels were identified by random forest analysis[85] and the percentage increases in the mean squared error (MSE) were used to estimate the importance of these indicators[86].

Relative abundance (RA) of a given taxonomic group per sample was calculated as the number of sequences affiliated with that group divided by the total number of sequences for a given sample. The significant differences in relative abundances of bacterial OTUs between DEHP and Control groups were determined both using LEfSe analysis[87] and Tukey's HSD test. The relative abundances of selected bacterial OTUs across different treatments were displayed using heatmap. Linear regression analyses relating pregnant rate to the bacterial diversity indices, bacterial phyla relative abundances and selected bacterial OTUs relative abundances were performed in basicTrendline package.

In order to find out relationships between different members of the intestinal bacterial microbiome and their potential combined influence on the pregnant rate and fertility related hormone levels, we constructed a network of cooccurring OTUs and further deconstructed the bacterial community into smaller coherent modules using weighted gene co-expression network analysis (WGCNA) method to inspect the specific relationships between different network modules with the pregnant rate and fertility related hormone levels[88].

Statistics

Statistical analyses were all carried out in R-4.2.1. The normality of the data was assessed using the Shapiro–Wilk test. For datasets that conformed to normal distribution, comparisons between groups were performed using Student's t test. In cases where the data did not meet the normality assumption, the Mann–Whitney U test, a non-parametric alternative, was employed. A p value of less than 0.05 was regarded as statistically significant[16].

Data availability

All raw sequences data are available in NCBI Sequence Read Archive (SRA) database under the accession number SRP452226. All code used in this study are available from the corresponding author on request.

Received: 5 September 2024; Accepted: 28 May 2025;
Published online: 13 June 2025

References

1. Martinez-Razo, L. D. et al. The impact of di-(2-ethylhexyl) phthalate and mono(2-ethylhexyl) phthalate in placental development, function, and pathophysiology. *Environ. Int.* **146**, 106228 (2021).
2. Jaakkola, J. J. & Knight, T. L. The role of exposure to phthalates from polyvinyl chloride products in the development of asthma and allergies: a systematic review and meta-analysis. *Environ. Health Perspect.* **116**, 845–853 (2008).
3. Shinohara, N. & Uchino, K. Diethylhexyl phthalate (DEHP) emission to indoor air and transfer to house dust from a PVC sheet. *Sci. Total Environ.* **711**, 134573 (2020).
4. Zhang, Y. et al. Oral intake exposure to phthalates in vegetables produced in plastic greenhouses and its health burden in Shaanxi province, China. *Sci. Total Environ.* **696**, 133921 (2019).
5. Fromme, H. et al. Intake of phthalates and di(2-ethylhexyl)adipate: results of the Integrated Exposure Assessment Survey based on duplicate diet samples and biomonitoring data. *Environ. Int.* **33**, 1012–1020 (2007).
6. Erythropel, H. C. et al. Leaching of the plasticizer di(2-ethylhexyl) phthalate (DEHP) from plastic containers and the question of human exposure. *Appl. Microbiol. Biotechnol.* **98**, 9967–9981 (2014).
7. Reddy, B. S. et al. Association of phthalate esters with endometriosis in Indian women. *BJOG* **113**, 515–520 (2006).
8. Barakat, R. et al. Prenatal exposure to DEHP induces premature reproductive senescence in male mice. *Toxicol. Sci.* **156**, 96–108 (2017).

9. Hannon, P. R. et al. Mono(2-ethylhexyl) phthalate accelerates early folliculogenesis and inhibits steroidogenesis in cultured mouse whole ovaries and antral follicles. *Biol. Reprod.* **92**, 120 (2015).
10. Agirman, G., Yu, K. B. & Hsiao, E. Y. Signaling inflammation across the gut-brain axis. *Science* **374**, 1087–1092 (2021).
11. Ahlawat, S., Asha & Sharma, K. K. Gut-organ axis: a microbial outreach and networking. *Lett. Appl. Microbiol.* **72**, 636–668 (2021).
12. Gubert, C. et al. Exercise, diet and stress as modulators of gut microbiota: implications for neurodegenerative diseases. *Neurobiol. Dis.* **134**, 104621 (2020).
13. Ku, T. et al. Tebuconazole mediates cognitive impairment via the microbe-gut-brain axis (MGBA) in mice. *Environ. Int.* **173**, 107821 (2023).
14. Sharma, T. et al. Gut microbiota: a non-target victim of pesticide-induced toxicity. *Gut Microbes* **15**, 2187578 (2023).
15. Serrano, S. E. et al. Phthalates and diet: a review of the food monitoring and epidemiology data. *Environ. Health* **13**, 43 (2014).
16. Fu, X. et al. Di-(2-ethylhexyl) phthalate exposure induces female reproductive toxicity and alters the intestinal microbiota community structure and fecal metabolite profile in mice. *Environ. Toxicol.* **36**, 1226–1242 (2021).
17. Diamante, G. et al. Systems toxicogenomics of prenatal low-dose BPA exposure on liver metabolic pathways, gut microbiota, and metabolic health in mice. *Environ. Int.* **146**, 106260 (2021).
18. Hirt, N. & Body-Malapel, M. Immunotoxicity and intestinal effects of nano- and microplastics: a review of the literature. *Part Fibre Toxicol.* **17**, 57 (2020).
19. Mikhael, S., Punjala-Patel, A. & Gavrilova-Jordan, L. Hypothalamic-pituitary-ovarian axis disorders impacting female fertility. *Biomedicines* **7** https://doi.org/10.3390/biomedicines7010005 (2019).
20. Stamatiades, G. A. & Kaiser, U. B. Gonadotropin regulation by pulsatile GnRH: signaling and gene expression. *Mol. Cell Endocrinol.* **463**, 131–141 (2018).
21. Maggi, R. et al. GnRH and GnRH receptors in the pathophysiology of the human female reproductive system. *Hum. Reprod. Update* **22**, 358–381 (2016).
22. Moeller-Gnangra, H. et al. ErbB4 point mutation in CU3 inbred rats affects gonadotropin-releasing-hormone neuronal function via compromised neuregulin-stimulated prostaglandin E2 release from astrocytes. *Glia* **67**, 309–320 (2019).
23. Prevot, V. et al. Function-related structural plasticity of the GnRH system: a role for neuronal-glial-endothelial interactions. *Front. Neuroendocrinol.* **31**, 241–258 (2010).
24. Liu, T. et al. Effects of di-(2-ethylhexyl) phthalate on the hypothalamus-pituitary-ovarian axis in adult female rats. *Reprod. Toxicol.* **46**, 141–147 (2014).
25. Ahmadpour, D., Mhaouty-Kodja, S. & Grange-Messent, V. Disruption of the blood-brain barrier and its close environment following adult exposure to low doses of di(2-ethylhexyl)phthalate alone or in an environmental phthalate mixture in male mice. *Chemosphere* **282**, 131013 (2021).
26. Aguilera, M., Galvez-Ontiveros, Y. & Rivas, A. Endobolome, a new concept for determining the influence of microbiota disrupting chemicals (MDC) in relation to specific endocrine pathogenesis. *Front. Microbiol.* **11**, 578007 (2020).
27. Xiao, W. et al. The microbiota-gut-brain axis participates in chronic cerebral hypoperfusion by disrupting the metabolism of short-chain fatty acids. *Microbiome* **10**, 62 (2022).
28. Zhang, J. et al. Probiotic bifidobacterium lactis V9 regulates the secretion of sex hormones in polycystic ovary syndrome patients through the gut-brain axis. *mSystems* **4** https://doi.org/10.1128/mSystems.00017-19 (2019).
29. Ervin, S. M. et al. Gut microbial beta-glucuronidases reactivate estrogens as components of the estrobolome that reactivate estrogens. *J. Biol. Chem.* **294**, 18586–18599 (2019).
30. Chen, X. et al. Hypothalamic mechanisms of obesity-associated disturbance of hypothalamic-pituitary-ovarian axis. *Trends Endocrinol. Metab.* **33**, 206–217 (2022).
31. Goldsammler, M., Merhi, Z. & Buyuk, E. Role of hormonal and inflammatory alterations in obesity-related reproductive dysfunction at the level of the hypothalamic-pituitary-ovarian axis. *Reprod. Biol. Endocrinol.* **16**, 45 (2018).
32. Murphy, V. E. et al. Endocrine regulation of human fetal growth: the role of the mother, placenta, and fetus. *Endocr. Rev.* **27**, 141–169 (2006).
33. Feldt-Rasmussen, U. & Mathiesen, E. R. Endocrine disorders in pregnancy: physiological and hormonal aspects of pregnancy. *Best. Pr. Res. Clin. Endocrinol. Metab.* **25**, 875–884 (2011).
34. Lee, S. G. et al. Bisphenol A exposure during adulthood causes augmentation of follicular atresia and luteal regression by decreasing 17beta-estradiol synthesis via downregulation of aromatase in rat ovary. *Environ. Health Perspect.* **121**, 663–669 (2013).
35. Dutta, S. et al. Reproductive toxicity of combined effects of endocrine disruptors on human reproduction. *Front. Cell Dev. Biol.* **11**, 1162015 (2023).
36. Wu, H. et al. Polystyrene-microplastics and DEHP co-exposure induced DNA damage, cell cycle arrest and necroptosis of ovarian granulosa cells in mice by promoting ROS production. *Sci. Total Environ.* **871**, 161962 (2023).
37. Liu, J. C. et al. Di (2-ethylhexyl) phthalate exposure impairs meiotic progression and DNA damage repair in fetal mouse oocytes in vitro. *Cell Death Dis.* **8**, e2966 (2017).
38. Chiang, C. & Flaws, J. A. Subchronic exposure to di(2-ethylhexyl) phthalate and diisononyl phthalate during adulthood has immediate and long-term reproductive consequences in female mice. *Toxicol. Sci.* **168**, 620–631 (2019).
39. Brehm, E. et al. Prenatal exposure to di(2-ethylhexyl) phthalate causes long-term transgenerational effects on female reproduction in mice. *Endocrinology* **159**, 795–809 (2018).
40. Bellavia, A. et al. Association between chemical mixtures and female fertility in women undergoing assisted reproduction in Sweden and Estonia. *Environ. Res.* **216**, 114447 (2023).
41. Radke, E. G. et al. Phthalate exposure and female reproductive and developmental outcomes: a systematic review of the human epidemiological evidence. *Environ. Int.* **130**, 104580 (2019).
42. Liu, J. C. et al. DEHP exposure to lactating mice affects ovarian hormone production and antral follicle development of offspring. *J. Hazard Mater.* **416**, 125862 (2021).
43. Cashion, A. B., Smith, M. J. & Wise, P. M. The morphometry of astrocytes in the rostral preoptic area exhibits a diurnal rhythm on proestrus: relationship to the luteinizing hormone surge and effects of age. *Endocrinology* **144**, 274–280 (2003).
44. Vanacker, C. et al. A role for glial fibrillary acidic protein (GFAP)-expressing cells in the regulation of gonadotropin-releasing hormone (GnRH) but not arcuate kisspeptin neuron output in male mice. *Elife* **10** https://doi.org/10.7554/eLife.68205 (2021).
45. Sharif, A., Baroncini, M. & Prevot, V. Role of glia in the regulation of gonadotropin-releasing hormone neuronal activity and secretion. *Neuroendocrinology* **98**, 1–15 (2013).
46. Garcia-Segura, L. M., Lorenz, B. & DonCarlos, L. L. The role of glia in the hypothalamus: implications for gonadal steroid feedback and reproductive neuroendocrine output. *Reproduction* **135**, 419–429 (2008).
47. Panatier, A. et al. Astrocytes are endogenous regulators of basal transmission at central synapses. *Cell* **146**, 785–798 (2011).

48. D'Ascenzo, M. et al. mGluR5 stimulates gliotransmission in the nucleus accumbens. *Proc. Natl Acad. Sci. USA* **104**, 1995–2000 (2007).
49. Harms, P. G., Ojeda, S. R. & McCann, S. M. Prostaglandin involvement in hypothalamic control of gonadotropin and prolactin release. *Science* **181**, 760–761 (1973).
50. Ma, Y. J. et al. Neuregulins signaling via a glial erbB-2-erbB-4 receptor complex contribute to the neuroendocrine control of mammalian sexual development. *J. Neurosci.* **19**, 9913–9927 (1999).
51. Prevot, V. et al. Normal female sexual development requires neuregulin-erbB receptor signaling in hypothalamic astrocytes. *J. Neurosci.* **23**, 230–239 (2003).
52. Ding, Z. et al. Neuregulin-1 converts reactive astrocytes toward oligodendrocyte lineage cells via upregulating the PI3K-AKT-mTOR pathway to repair spinal cord injury. *Biomed. Pharmacother.* **134**, 111168 (2021).
53. Yu, D. et al. Prenatal di-(2-ethylhexyl) phthalate exposure induced myocardial cytotoxicity via the regulation of the NRG1-dependent ErbB2/ErbB4-PI3K/AKT signaling pathway in fetal mice. *Ecotoxicol. Environ. Saf.* **241**, 113771 (2022).
54. Singh, P. et al. Maternal microbiota and gestational diabetes: impact on infant health. *J. Transl. Med.* **21**, 364 (2023).
55. Zhao, Y. et al. The effect of gut microbiota dysbiosis on patients with preeclampsia. *Front. Cell Infect. Microbiol.* **12**, 1022857 (2022).
56. Chiang, C. et al. Exposure to di(2-ethylhexyl) phthalate and diisononyl phthalate during adulthood disrupts hormones and ovarian folliculogenesis throughout the prime reproductive life of the mouse. *Toxicol. Appl. Pharm.* **393**, 114952 (2020).
57. Hu, X. et al. Gut microbiota dysbiosis promotes the development of epithelial ovarian cancer via regulating Hedgehog signaling pathway. *Gut Microbes* **15**, 2221093 (2023).
58. Shin, J. et al. Ageing and rejuvenation models reveal changes in key microbial communities associated with healthy ageing. *Microbiome* **9**, 240 (2021).
59. Belda, E. et al. Impairment of gut microbial biotin metabolism and host biotin status in severe obesity: effect of biotin and prebiotic supplementation on improved metabolism. *Gut* **71**, 2463–2480 (2022).
60. Hu, S. et al. Gut microbial beta-glucuronidase: a vital regulator in female estrogen metabolism. *Gut Microbes* **15**, 2236749 (2023).
61. Zhang, J. et al. Microbial enzymes induce colitis by reactivating triclosan in the mouse gastrointestinal tract. *Nat. Commun.* **13**, 136 (2022).
62. Ning, L. & Hong, J. Gut microbial beta-glucuronidase: a key regulator of endobiotic homeostasis. *Cell Host Microbe* **32**, 783–785 (2024).
63. Kloting, N. et al. Di-(2-ethylhexyl)-phthalate (DEHP) causes impaired adipocyte function and alters serum metabolites. *PLoS ONE* **10**, e0143190 (2015).
64. Li, T. T. et al. Polyunsaturated fatty acids from microalgae Spirulina platensis modulates lipid metabolism disorders and gut microbiota in high-fat diet rats. *Food Chem. Toxicol.* **131**, 110558 (2019).
65. Watts, N. et al. Health and climate change: policy responses to protect public health. *Lancet* **386**, 1861–1914 (2015).
66. Hanson, M. & Muller, R. Epigenetic inheritance and the responsibility for health in society. *Lancet Diabetes Endocrinol.* **5**, 11–12 (2017).
67. Nadeau, J. H. & Topol, E. J. The genetics of health. *Nat. Genet.* **38**, 1095–1098 (2006).
68. Altorok, N. & Kahaleh, B. Epigenetics and systemic sclerosis. *Semin. Immunopathol.* **37**, 453–462 (2015).
69. Park, S. K. et al. Environmental cadmium and mortality from influenza and pneumonia in U.S. adults. *Environ. Health Perspect.* **128**, 127004 (2020).
70. Countdown to 2030 Collaboration. Countdown to 2030: tracking progress towards universal coverage for reproductive, maternal, newborn, and child health. *Lancet* **391**, 1538–1548 (2018).
71. Aizer, A. & Currie, J. The intergenerational transmission of inequality: maternal disadvantage and health at birth. *Science* **344**, 856–861 (2014).
72. Li, N. et al. Role of the 17beta-hydroxysteroid dehydrogenase signalling pathway in di-(2-ethylhexyl) phthalate-induced ovarian dysfunction: an in vivo study. *Sci. Total Environ.* **712**, 134406 (2020).
73. Ku, T. et al. Tebuconazole induces liver injury coupled with ROS-mediated hepatic metabolism disorder. *Ecotoxicol. Environ. Saf.* **220**, 112309 (2021).
74. Olofsson, L. E. et al. Modulation of AgRP-neuronal function by SOCS3 as an initiating event in diet-induced hypothalamic leptin resistance. *Proc. Natl Acad. Sci. USA* **110**, E697–E706 (2013).
75. Paone, P. et al. Prebiotic oligofructose protects against high-fat diet-induced obesity by changing the gut microbiota, intestinal mucus production, glycosylation and secretion. *Gut Microbes* **14**, 2152307 (2022).
76. Claesson, M. J. et al. Comparative analysis of pyrosequencing and a phylogenetic microarray for exploring microbial community structures in the human distal intestine. *PLoS ONE* **4**, e6669 (2009).
77. Edgar, R. C. UPARSE: highly accurate OTU sequences from microbial amplicon reads. *Nat. Methods* **10**, 996–998 (2013).
78. Wang, Q. et al. Naive Bayesian classifier for rapid assignment of rRNA sequences into the new bacterial taxonomy. *Appl. Environ. Microbiol.* **73**, 5261–5267 (2007).
79. Khan, M. H. et al. Fecal beta-glucuronidase activity differs between hematopoietic cell and kidney transplantation and a possible mechanism for disparate dose requirements. *Gut Microbes* **14**, 2108279 (2022).
80. Faith, D. P. Conservation evaluation and phylogenetic diversity. *Biol. Conserv.* **61**, 1–10 (1992).
81. Schloss, P. D. et al. Introducing mothur: open-source, platform-independent, community-supported software for describing and comparing microbial communities. *Appl. Environ. Microbiol.* **75**, 7537–7541 (2009).
82. Oksanen, J. et al. Vegan: Community Ecology Package. R package version 2.0-4. (2012).
83. Anderson, M. J. A new method for non-parametric multivariate analysis of variance. *Austral Ecol.* **26**, 32–46 (2001).
84. De'ath, G. Multivariate regression trees: a new technique for modeling species-environment relationships. *Ecology* **83**, 1105–1117 (2002).
85. Jin, T. et al. Taxonomic structure and functional association of foxtail millet root microbiome. *Gigascience* **6**, 1–12 (2017).
86. Jiao, S. et al. Soil microbiomes with distinct assemblies through vertical soil profiles drive the cycling of multiple nutrients in reforested ecosystems. *Microbiome* **6**, 146 (2018).
87. Segata, N. et al. Metagenomic biomarker discovery and explanation. *Genome Biol.* **12**, R60 (2011).
88. Org, E. et al. Relationships between gut microbiota, plasma metabolites, and metabolic syndrome traits in the METSIM cohort. *Genome Biol.* **18**, 70 (2017).

Acknowledgements

This research was supported by the Natural Science Foundation of Jiangsu Province, China (BK20230153), Nanjing Medical Science and Technology Development Foundation (ZKX14035) and Jiangsu Province Capability Improvement Project through Science, Technology and Education Jiangsu Provincial Medical Key Discipline (ZDXK202211).

Author contributions

Data curation and visualization: L.X., J.Y., and T.Y.; Writing—original draft: L.X.; Conceptualization: L.X. and H.D.; Formal analysis: J.Y., L.X., T.Y., and Y.P.; Methodology: M.C., X.W., and L.W. The authors read and approved the final manuscript.

Competing interests
The authors declare no competing interests.

Ethical approval
The animal experiments were approved by the Institutional Animal Care and Use Committee of Nanjing Medical University (Approval Number IACUC-2112042).

Additional information
Supplementary information The online version contains supplementary material available at https://doi.org/10.1038/s41522-025-00742-6.

Correspondence and requests for materials should be addressed to Linjie Xu or Hongjuan Ding.